A Quantum Mechanical/Molecular Mechanical Study of the Hydroxylation of Phenol and Halogenated Derivatives by Phenol Hydroxylase

Lars Ridder,*,[†] Adrian J. Mulholland,[‡] Ivonne M. C. M. Rietjens,[†] and Jacques Vervoort[†]

Contribution from the Laboratory of Biochemistry, Wageningen University, Dreijenlaan 3, 6703 HA Wageningen, The Netherlands, and School of Chemistry, University of Bristol, Bristol BS8 1TS, U.K.

Abstract: A combined quantum mechanical and molecular mechanical (QM/MM) method (AM1/CHARMM) was used to investigate the mechanism of the aromatic hydroxylation of phenol by a flavin dependent phenol hydroxylase (PH), an essential reaction in the degradation of a wide range of aromatic compounds. The model for the reactive flavin intermediate (C4a-hydroperoxyflavin) bound to PH was constructed on the basis of the crystal structure of the enzyme–substrate complex. A potential energy surface (PES) was calculated as a function of the reaction coordinates for hydroxylation of phenol (on C6) and for proton transfer from phenol (O1) to an active-site base Asp54 (OD1). The results support a reaction mechanism in which phenol is activated through deprotonation by Asp54, after which the phenolate is hydroxylated through an electrophilic aromatic substitution. Ab initio test calculations were performed to verify these results of the QM/MM model. Furthermore, the variation in the calculated QM/MM activation energies for hydroxylation of a series of substrate derivatives was shown to correlate very well ($R = 0.98$) with the natural logarithm of the experimental rate constants for their overall conversion by PH (25 °C, pH 7.6). This correlation validates the present QM/MM model and supports the proposal of an electrophilic aromatic substitution mechanism in which the electrophilic attack of the C4a-hydroperoxyflavin cofactor on the activated (deprotonated) substrate is the rate-limiting step at 25 °C and pH 7.6. The correlation demonstrates the potential of the QM/MM technique for predictions of catalytic activity on the basis of protein structure. Analysis of the residue contributions identifies a catalytic role for the backbone carbonyl of a conserved proline residue, Pro364, in specific stabilization of the transition state for hydroxylation. A crystal water appears to assist in the hydroxylation reaction by stabilizing the deprotonated C4a-hydroxyflavin product. Comparison of the present results with previous QM/MM results for the related *p*-hydroxybenzoate hydroxylase (Ridder et al. *J. Am. Chem. Soc.* **1998**, *120*, 7641–7642) identifies common mechanistic features, providing detailed insight into the relationship between these enzymes.

Introduction

Flavin-dependent phenol hydroxylase (PH) catalyzes the hydroxylation of phenol, specifically at the *ortho* position. This is an important step in the microbial degradation pathway of aromatic compounds including lignin, the main constituent of wood and therefore one of the most abundant natural compounds. The PH reaction leads to the formation of catechol, the aromatic ring of which can be cleaved subsequently by catechol dioxygenases. In addition to the parent substrate, various substituted phenols are hydroxylated by the enzyme, including fluorophenols, chlorophenols, aminophenols, nitrophenols, dihydroxybenzenes, and cresol.[1–3] As a result, the reactions catalyzed by PH are also important for degradation and detoxification of a large group of aromatic pollutants of industrial origin.

Transient kinetic studies on phenol hydroxylase[4] support a catalytic mechanism which proceeds via a C4a-hydroperoxy-flavin intermediate, formed by reduction of the FAD cofactor by NADPH, subsequent incorporation of molecular oxygen and protonation of the resulting peroxide moiety. The C4a-hydroperoxyflavin is proposed to react with the phenolic substrate via an electrophilic aromatic substitution mechanism, which results in the formation of a cyclohexadienone as the initial reaction product. The cyclohexadienone is converted non-enzymatically into the catechol product via keto–enol tautomerisation.[4]

Theoretical analysis on the basis of the 3D structure of enzymes is becoming increasingly important in providing additional information on their reaction mechanisms.[5–9] A powerful approach to simulate reactions within large molecular systems is to combine quantum mechanical (QM) and molecular mechanical (MM) methods. The combined QM/MM approach allows the part of the system directly involved in the chemical reaction to be described by quantum mechanics, while the

[†] Wageningen University.
[‡] University of Bristol.
(1) Peelen, S.; Rietjens, I. M. C. M.; Boersma, M. G.; Vervoort, J. *Eur. J. Biochem.* **1995**, *227*, 284–291.
(2) Neujahr, H. Y.; Gaal, A. *Eur. J. Biochem.* **1973**, *35*, 386–400.
(3) Gaal, A.; Neujahr, H. Y. *J. Bacteriology* **1979**, *137*, 13–21.
(4) Maeda-Yorita, K.; Massey, V. *J. Biol. Chem.* **1993**, *268*, 4134–4144.

(5) Warshel, A.; Levitt, M. *J. Mol. Biol.* **1976**, *103*, 227–249.
(6) Bash, P. A.; Field, M. J.; Davenport, R. C.; Petsko, G. A.; Ringe, D.; Karplus, M. *Biochemistry* **1991**, *30*, 5826–5832.
(7) Mulholland, A. J.; Richards, W. G. *Proteins* **1997**, *27*, 9–25.
(8) Harrison, M. J.; Burton, N. A.; Hillier, I. H. *J. Am. Chem. Soc.* **1997**, *119*, 12285–12291.
(9) Ridder, L.; Mulholland, A. J.; Vervoort, J.; Rietjens, I. M. C. M. *J. Am. Chem. Soc.* **1998**, *120*, 7641–7642.

environment is described by (computationally cheaper) molecular mechanics. In previous studies,[9,10] a QM/MM approach was used to study the aromatic hydroxylation step catalyzed by *p*-hydroxybenzoate hydroxylase (PHBH), which is both structurally and functionally related to PH.[4,11] This QM/MM simulation provided detailed insight into the electrophilic attack of the C4a-hydroperoxyflavin on the substrate, catalyzed by PHBH, and the importance of substrate activation through its deprotonation.

In the present study, the equivalent step in the reaction cycle of phenol hydroxylase is investigated by a similar QM/MM approach, which was shown to be valid and useful for this type of reaction in our previous study.[9] The first objective was to study the reaction mechanism of hydroxylation in PH in atomic detail, to identify some important catalytic features. A comparison of the results obtained for PH with the results of our earlier studies on the homologous step in PHBH provides detailed insight into some remarkable similarities as well as some intriguing differences in the structure and function of these two related enzymes. The second objective was to investigate whether the energy barriers calculated for the hydroxylation step by PH could be related quantitatively to experimental overall rate constants for the conversion of a series of phenol derivatives.[1] Such correlations are important to assess the potential of QM/MM simulations for the prediction of the catalytic properties of enzymes with respect to new substrates.[9]

An unanswered question about the mechanism of hydroxylation in PH is how substrate is activated toward reaction with the hydroperoxyflavin cofactor, the key step in the hydroxylation process. For PHBH, a number of studies[12-14] provide evidence for a mechanism in which the hydroxyl moiety of the substrate becomes deprotonated upon binding, which activates the substrate for an electrophilic attack by the hydroperoxyflavin.[15] The previous simulation of this reaction step indicated that deprotonation of the substrate does indeed significantly lower the activation energy for hydroxylation.[9,10] It is not clear whether a similar deprotonation of substrate occurs in phenol hydroxylase. NMR experiments indicate that the substrate binds to the oxidized PH enzyme in its neutral protonated state.[16] However, in analogy to results previously obtained for PHBH,[10] the protonation state of the phenol substrate in the active site is expected to influence its susceptibility to electrophilic attack by the C4a-hydroperoxyflavin. The crystal structure of PH indicates the presence of a hydrogen bond between the hydroxyl moiety of the substrate and a potential active-site base, Asp54. Therefore, the possibility of proton transfer from the phenol substrate molecule to Asp54 was included in the present simulation.

Methods

Construction of the Protein Model for The C4a-hydroperoxyflavin Intermediate of Phenol Hydroxylase. The crystal structure of PH from *Trichosporon cutaneum* in complex with substrate[11] (PDB entry code 1FOH) contains two homodimers in the oxidized state. In each dimer, two different conformations of the flavin are present in the two monomers: the so-called "in" (chains C and D) and "out" (chains A and B) conformations. In analogy to the conclusions of a number of studies on PHBH[17-19] the "in" conformation is expected to represent the conformation in which substrate hydroxylation can occur. Therefore, one of the subunits in the crystal structure in which the flavin is in the "in" conformation (chain C) was chosen as the starting point for building a model for the C4a-hydroperoxyflavin intermediate of phenol hydroxylase in complex with substrate. The model consists of all protein atoms of the monomer, in which the active site is completely buried, and inaccessible to solvent.[11] The flavin cofactor, present in the crystal structure in its oxidized state, was modified to the reactive C4a-hydroperoxyflavin intermediate by superimposing coordinates of an experimentally derived model of the C4a-hydroperoxyflavin,[19-21] using the algorithm of Kabsch[22] implemented by Schreuder et al.[19] Forty crystallographic waters within a 16 Å sphere around the distal oxygen of the C4a-hydroperoxyflavin were included. Hydrogen atoms on these crystal water molecules were built using the HBUILD routine in the CHARMM molecular mechanics package version 24b1.[23]

Several ionizable side chains are present in the active site of phenol hydroxylase. A correct assignment of charges on ionizable side chains is of importance for the QM/MM calculations described below, since the MM point charges influence the electron density distribution in the QM system. Information about protonation states of ionizable side chains is not directly provided by the crystal structure. Histidine side chains are a particular problem as their pK_a's can have values below and above the physiological pH, dependent on the specific protein environment. The protonation states of four active site histidines in PH, His116, His189, His 360, and His362, were selected essentially as described by Mulholland and Richards.[7] The various possible protonation states were tested by applying (QM/MM) geometry optimization as described in the next section. All four histidines remained closest to their crystal coordinates when treated in their neutral states with a proton on NE1. These neutral states were therefore used in further calculations. Likewise, when Lys365 was treated as protonated, the structure became altered due to a hydrogen bond interaction (not present in the crystal structure) between the charged Lys365 side chain and the backbone carbonyl of Pro364. Lys365 was therefore modeled in its neutral state in which it kept its crystal structure conformation (being a good hydrogen bond acceptor for Tyr336).

An essential aspect of the model is the protonation state of phenol and of two residues with which the hydroxyl group of phenol appears to form hydrogen bonds, Asp54 and Tyr289. It is expected that these hydrogen bonds in the crystal structure of the oxidized state are also present during the hydroxylation step. Furthermore, the presence of the two hydrogen bonds would imply that (only) one of the three ionizable groups could be deprotonated. Since Asp54 is potentially the most acidic of the three, the electronic state with a deprotonated Asp54 (Figure 1) is chosen as the initial model. However, deprotonation of phenol would be expected to activate this substrate for the electrophilic attack by the C4a-hydroperoxyflavin. Therefore, the possibility of proton transfer from phenol to Asp54 was included in the subsequent simulations. For this reason, part of the Asp54 side chain was included in the quantum mechanical region of the model as described in the next section. The situation in which Tyr289 is deprotonated is considered unlikely to be of physiological relevance and was therefore not investigated.

(10) Ridder, L.; Mulholland, A. J.; Rietjens, I. M. C. M.; Vervoort, J. *J. Mol. Graphics Modell.* **1999**, *17*, 163−175.

(11) Enroth, C.; Neujahr, H.; Schneider, G.; Lindqvist, Y. *Structure* **1998**, *6*, 605−617.

(12) Entsch, B.; Ballou, D. P.; Massey, V. *J. Biol. Chem.* **1976**, *251*, 2550−2563.

(13) Entsch, B.; Palfey, B. A.; Ballou, D. P.; Massey, V. *J. Biol. Chem.* **1991**, *266*, 17341−17349.

(14) Eschrich, K.; Van Der Bolt, F. J. T.; De Kok, A.; Van Berkel, W. J. H. *Eur. J. Biochem.* **1993**, *216*, 137−146.

(15) Vervoort, J.; Rietjens, I. M. C. M.; Van Berkel, W. J. H.; Veeger, C. *Eur. J. Biochem.* **1992**, *206*, 479−484.

(16) Peelen, S.; Rietjens, I. M. C. M.; Van Berkel, W. J. H.; Van Workum, W. A.; Vervoort, J. *Eur. J. Biochem.* **1993**, *218*, 345−353.

(17) Gatti, D. L.; Palfey, B. A.; Lah, M. S.; Entsch, B.; Massey, V.; Ballou, D. P.; Ludwig, M. L. *Science* **1994**, *266*, 110−113.

(18) Schreuder, H. A.; Mattevi, A.; Obmolova, G.; Kalk, K. H.; Hol, W. G.; Van der Bolt, F. J.; Van Berkel, W. J. *Biochemistry* **1994**, *33*, 10161−10170.

(19) Schreuder, H. A.; Hol, W. G. J.; Drenth, J. *Biochemistry* **1990**, *29*, 3101−3108.

(20) Bolognesi, M.; Ghisla, S.; Incoccia, L. *Acta Crystallogr., Sect. B* **1978**, *34*, 821−828.

(21) Vervoort, J.; Müller, F.; Lee, J.; Moonen, C. T. W.; Van den Berg, W. A. M. *Biochemistry* **1986**, *25*, 8062−8067.

(22) Kabsch, W. *Acta Crystallogr., Sect. A* **1976**, *32*, 922−923.

(23) Brooks, B. R.; Bruccoleri, R. E.; Olafson, B. D.; States, D. J.; Swaminathan, S.; Karplus, M. *J. Comput. Chem.* **1983**, *4*, 187−217.
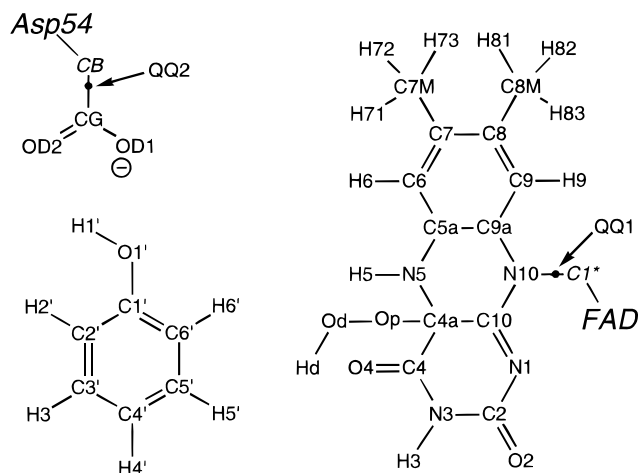
Figure 1. The QM region of the present model for the C4a-hydroperoxyflavin intermediate in the PH reaction cycle. MM atoms are labeled in italics. Bonds crossing the QM/MM boundary are replaced by bonds to link atoms,[27] QQ1 and QQ2, in the QM system.

Application of the AM1/CHARMm 22 QM/MM Potential. The flavin ring, the substrate, and the side chain of Asp54 (a total of 49 atoms) were treated quantum mechanically (Figure 1) with the semiempirical (closed shell) AM1 Hamiltonian.[24,25] All other atoms of the complete subunit (6628) were treated at the molecular mechanical level, using the CHARMm 22 "united atom" force field (polar hydrogens only).[26] Two types of nonbonded interactions between the QM and MM atoms are accounted for. Classical VDW terms are used to include steric effects between the QM and MM atoms, whereas the electronic interactions are accounted for by including the MM point charges (as atomic "cores") in the Hamiltonian for the QM system.[27] The covalent bonds, which cross the boundary between the QM and MM regions, were treated by introducing so-called link atoms, which are included in the QM system as hydrogen atoms.[27] The same QM/MM potential has been applied successfully in previous studies.[7,9,10] The QM region has a total charge of $-1e$. A dielectric constant of 1.0 was used for all MM and QM/MM electrostatic interactions. An approximate correction for dielectric screening in the MM and QM/MM electrostatic interactions was applied through the use of a 16 Å nonbonded cutoff. The electrostatic interactions were smoothly scaled down to zero over the 11 to 16 Å distance range, using a group-based switching function.[23] All QM atoms were treated as one group to ensure that the MM charges were treated consistently in the Hamiltonian for the QM atoms, that is, all QM atoms "feel" the same MM charges.

Throughout the calculations, all atoms within a 16 Å active-site region around the distal oxygen of the C4a-hydroperoxyflavin (Od) were optimized. Atoms outside this active site region were fixed. All non-hydrogen atoms within a 14 Å to 16 Å buffer-zone were harmonically restrained to their crystal coordinates with force constants based on model average *B*-factors[28] and scaled from zero at 14 Å to maximum at 16 Å away from the center of the active site region (Od).

Definition of the Reaction Coordinates for Hydroxylation and Proton Transfer to Asp54. The two reaction coordinates of interest are the electrophilic attack of the distal oxygen Od of the C4a-hydroperoxyflavin on the substrate and the proton transfer from O1′ of the substrate to OD1 of Asp54. In the PH structure, the position of one of the two carbon centers (C6′ in the crystal structure) *ortho* with respect to the hydroxyl moiety is much closer to the distal oxygen of the flavin peroxide than the other (C2′ in the crystal structure). Therefore, only the electrophilic attack of the distal oxygen of the

cofactor on the C6′ position of the substrate was assumed to be of physiological relevance. The reaction coordinate for this step (r_{OH}) was defined as $r_{OH} = d(Op-Od) - d(Od-C6')$. This definition of the reaction coordinate is identical to the definition successfully used in a previous simulation of the equivalent reaction step in PHBH.[10] The reaction coordinate (r_H) for proton transfer from the O1′ of phenol to OD1 of Asp54 was defined as $r_H = d(O1'-H1') - d(H1'-OD1)$. The reaction coordinate restraints were applied using the CHARMM RESDistance command.[29]

Initial Optimization and Solvation of the Simulation System. The QM/MM model was initially optimized with the two reaction coordinates of interest harmonically restrained ($k = 5000$ kcal mol^{-1} Å^{-2}) to their midpoint values, that is, $r_{OH} = r_H = 0$, which is equivalent to $d(Op-Od) = d(Od-C6')$ and $d(O1'-H1') = d(H1'-OD1)$. This required 1281 steps of ABNR minimization (gradient < 0.01 kcal mol^{-1} Å^{-1}). The structure thus obtained represents a midpoint of the potential energy surface to be calculated as described in the next section. This midpoint structure was first solvated as follows. Fifteen water molecules were added by superimposing an equilibrated box of TIP3P waters and removing all waters further than 16 Å away from the center of the active site region or having an oxygen atom within 2.6 Å of another non-hydrogen atom. To equilibrate the solvent (including crystal waters) within the protein, 26 ps of stochastic boundary molecular dynamics (SBMD)[28] were performed at 300 K with the protein atoms fixed (at their optimized positions) and with MM point charges on the QM atoms derived from a fit to the (AM1) electrostatic potential around the isolated QM atoms.[30] Cooling from 300 to 0 K was performed during another 6 ps of SBMD. The solvation procedure (superimposing an equilibrated box of TIP3P waters and removing all waters further than 16 Å away from the center of the active-site region or having an oxygen atom within 2.6 Å of another non-hydrogen atom) was then repeated, resulting in the addition of three more water molecules. In a next step, 250 steps of ABNR minimization were applied to optimize the positions of the water molecules within the (frozen) protein.

This solvated system was again fully optimized (gradient < 0.01 kcal mol^{-1}Å^{-1}, requiring 1046 steps of ABNR minimization) with all the active site atoms free to move, using the boundary and reaction coordinate restraints and the QM/MM potential as described above. The complete model consisted of substrate, the C4a-hydroperoxide form of FAD, all 656 amino acid residues, 40 crystal water molecules and 18 newly built water molecules.

Calculation of a Potential Energy Surface. Starting from this solvated QM/MM model a potential energy surface was calculated on a grid by restraining the two reaction coordinates. The reaction coordinate for hydroxylation (r_{OH}) was harmonically restrained with a force constant of $k = 5000$ kcal mol^{-1} Å^{-2}, and was varied between -2.0 and $+2.0$ Å in steps of 0.2 Å. The reaction coordinate for proton transfer (r_H) was harmonically restrained, using the same force constant as used for restraining the hydroxylation reaction, and was varied between -1.0 and $+1.4$ Å. All water atoms were harmonically restrained to their initial optimized positions, using a mass-weighted force constant of 0.1 kcal mol^{-1} Å^{-2} to prevent discontinuous changes in the solvent configuration. At each gridpoint, up to 303 steps of ABNR minimization were performed, starting from the geometry of a neighboring grid point, until the gradient became less than 0.02 kcal mol^{-1} Å^{-1}. The approximate stationary points on the surface, that is, minima (corresponding to intermediates) and saddle points (corresponding to approximate transition states), were determined more precisely by performing additional geometry optimizations with only one (for saddle points) or neither (for minima) of the reaction coordinates restrained. The reaction coordinate values that correspond to the approximate transition states r(TS) were determined to 0.01 Å precision.

Validation of the AM1 Method. The present QM/MM model treats the substrate, the flavin ring and the carboxylate moiety of the active site base, Asp54 quantum mechanically (Figure 1), using the semiempirical AM1 method. To test the adequacy of this semiempirical method

(24) Dewar, M. J. S.; Zoebisch, E. G.; Healy, E. F.; Stewart, J. J. P. *J. Am. Chem. Soc.* **1985**, *107*, 3902−3909.

(25) Dewar, M. J. S.; Zoebisch, E. G. *J. Mol. Struct. (THEOCHEM)* **1988**, *180*, 1−21.
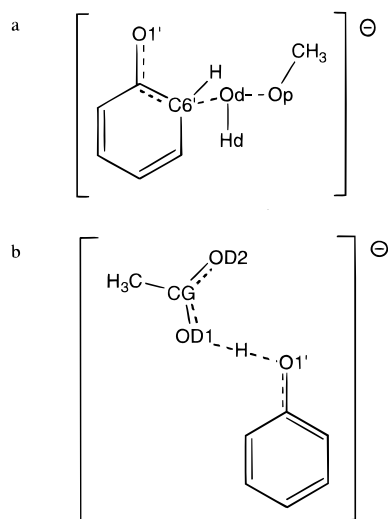
(26) QUANTA 1993; Molecular Simulations Inc.: 200 Fifth Ave., Waltham, MA, 1993.

(27) Field, M. J.; Bash, P. A.; Karplus, M. *J. Comput. Chem.* **1990**, *11*, 700−733.

(28) Brooks, C. L., III; Karplus, M. *J. Mol. Biol.* **1989**, *208*, 159−181.

(29) Eurenius, K. P.; Chatfield, D. C.; Brooks, B. R.; Hodoscek, M. *Int. J. Quantum Chem.* **1996**, *60*, 1189−1200.

(30) SPARTAN, v5.1; Wave Function Inc.: 18401 Von Karman Avenue, Suite 370, Irvine, CA 92612.

Figure 2. Transition state models (a) for the hydroxylation reaction in which the C4a-hydroperoxyflavin cofactor is replaced by methylperoxide, and (b) for proton transfer from phenol to Asp54.

for the reactions of interest, its performance for small model systems was compared to higher level ab initio methods. For the hydroxylation reaction a model system was investigated in which the C4a-hydroperoxyflavin is replaced by methyl peroxide (Figure 2a). The second reaction of interest, proton transfer from phenol to Asp54, was tested with a small model system consisting of phenol and acetic acid (Figure 2b). Reactants, transition states, and products were optimized in the gas phase using Gaussian98[31] and Spartan 5.1.[30] The AM1 results are compared to results from ab initio HF and MP2 calculations and density functional B3LYP calculations using the 6-31+G(d) basis set.

Amino Acid Decomposition Analysis. To identify important active-site residues, an energy decomposition analysis was performed, with a procedure similar to those used previously.[6,7,10,32,33] The contributions of individual MM residues to the total QM/MM energy barriers, and to the energy differences between the reactant and product states, were determined for the proton transfer as well as the hydroxylation reaction. The analyses start from the energy difference between the reactant and the transition states, or the reactant and the product states, without the MM protein environment included. Then, one by one, the amino acid residues are included in the energy difference calculation in order of increasing distance between their center of mass (COM) and the distal oxygen of the hydroperoxyflavin. The effect of an (MM) residue on the total QM/MM energy difference gives an approximate and qualitative indication of its influence on the energy of the reaction in the active site of PH.

Calculation of Energy Barriers for Substituted Phenols. In addition to the calculations with the native substrate, relevant points on the potential energy surface, that is, the phenolate and transition-state complexes, were calculated for a series of 15 phenol derivatives with fluoro- and chloro-substituents, which are known to be substrates for PH.[1] These calculations started from the relevant structures obtained for phenol, in which phenol was replaced by the substituted substrates.

(31) Frisch, M. J.; Trucks, G. W.; Schlegel, H. B.; Scuseria, G. E.; Robb, M. A.; Cheeseman, J. R.; Zakrzewski, V. G.; Montgomery, J. A. J.; Stratmann, R. E.; Burant, J. C.; Dapprich, S.; Millam, J. M.; Daniels, A. D.; Kudin, K. N.; Strain, M. C.; Farkas, O.; Tomasi, J.; Barone, V.; Cossi, M.; Cammi, R.; Mennucci, B.; Pomelli, C.; Adamo, C.; Clifford, S.; Ochterski, J.; Petersson, G. A.; Ayala, P. Y.; Cui, Q.; Morokuma, K.; Malick, D. K.; Rabuck, A. D.; Raghavachari, K.; Foresman, J. B.; Cioslowski, J.; Ortiz, J. V.; Stefanov, B. B.; Liu, G.; Liashenko, A.; Piskorz, P.; Komaromi, I.; Gomperts, R.; Martin, R. L.; Fox, D. J.; Keith, T.; Al-Laham, M. A.; Peng, C. Y.; Nanayakkara, A.; Challacombe, M.; Gill, P. M. W.; Johnson, B.; Chen, W.; Wong, M. W.; Andres, J. L.; Gonzalez, C.; Head-Gordon, M.; Replogle, E. S.; Pople, J. A. *Gaussian98,* revision A.6; Gaussian, Inc.: Pittsburgh, PA, 1998.
(32) Lyne, P.; Mulholland, A. J.; Richards, W. G. *J. Am. Chem. Soc.* **1995**, *117*, 11345–11350.
(33) Cunningham, M. A.; Ho, L. L.; Nguyen, D. T.; Gillilan, R. E.; Bash, P. A. *Biochemistry* **1997**, *36*, 4800–4816.

QM/MM energy minimization was applied using the same geometry restraints as used for phenol. For the transition state, the reaction coordinate r_{OH} was varied to find the approximate transition-state to 0.01 Å accuracy with respect to r_{OH} (similar to the procedure with the native substrate). The energy barriers were calculated as the energy difference between the reactant and transition state structures thus obtained. For the asymmetrically substituted substrates these calculations were performed for the two possible orientations.

Correlation of Calculated Energy Barriers with Experimental Rate Constants. The calculated QM/MM energy barriers were compared with experimental rate constants for enzymatic conversion of the different phenols by PH.[1] [Four of the substrate derivatives investigated by Peelen et al.[1] were not included in the present study. The $K_M(NADPH)$ values with these substrates appeared to be significantly higher than with the other substrates which makes the k_{cat} values derived from these experiments (with [NADPH] < $K_M(NADPH)$) inaccurate.] On the basis of the Arrhenius equation, a linear correlation of the natural logarithm of the experimental rate constants with the calculated barriers is expected, if the hydroxylation step is indeed rate-limiting:

$$k_{cat} = A\ e^{-E_{act}/RT} \leftrightarrow \ln k_{cat} \propto -E_{act}$$

In the case of the asymmetric substrates two different orientations of the substrate, and therefore two different reactions, are relevant. For these substrates, the average values of the two calculated energy barriers were used in the correlation with the logarithm of the experimental rate constants for overall conversion.[1] A more sophisticated approach to calculate apparent energy barriers, based on the calculated barriers for the two orientations and on experimental product ratios, is given in the Supporting Information.

Results

Potential Energy Surface. Figure 3 presents the QM/MM potential energy surface as a function of both reaction coordinates, obtained from the grid of geometry optimizations. From the potential energy surface six approximate stationary points were identified and determined more precisely by performing additional geometry optimizations: the phenol complex, the transition state for proton transfer (TS_{proton}), the phenolate complex, the transition states for hydroxylation of phenol (TS_{phenol}) and phenolate ($TS_{phenolate}$), and the cylcohexadienone product complex (Figure 4).

The product complex, in which H1′ is on Asp54, is the most stable state on the calculated energy surface. This indicates that the proton H1′ does indeed shift from phenol to Asp54 somewhere in the overall reaction. It is apparent that the potential energy surface does not support a concerted mechanism, that is, a mechanism in which hydroxylation and proton transfer occur at the same time. This would be the case if a single transition state (e.g., a saddle point in the center region of the potential energy surface in Figure 3) connected the phenol−C4a-hydroperoxyflavin complex to the deprotonated cyclohexadienone−C4a-hydroxyflavin complex. Instead, two stepwise reaction pathways are possible. One possible reaction pathway is the hydroxylation of the neutral phenol, directly followed by transfer of a proton from the product to Asp54. In the alternative reaction pathway, first the proton H1′ from the hydroxyl moiety of phenol is transferred to Asp54, after which hydroxylation of the phenolate takes place.

Table 1 presents the energies, relative to the phenol complex, and some important atomic distances in the various optimized structures. It can be seen from Table 1 that direct hydroxylation of phenol corresponds to an energy barrier of about 36 kcal/mol. It is apparent from Figure 3 that the direct hydroxylation of phenol itself does not result in an intermediate (i.e., a minimum) with the H1′ still on O1′ (represented by the scheme
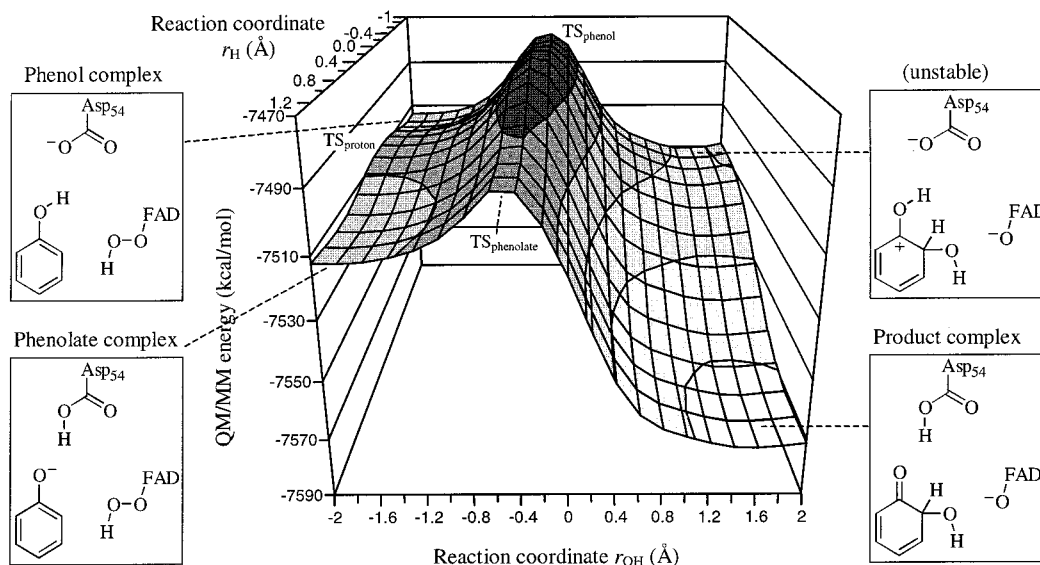
Figure 3. QM/MM potential energy surface as a function of the two reaction coordinates $r_{OH} = d(Op-Od) - d(Od-C6')$ and $r_H = d(O1'-H1') - d(H1'-OD1_{Asp54})$, obtained by interpolation of the energies of all optimized intermediate structures (using Microsoft Excel 97).
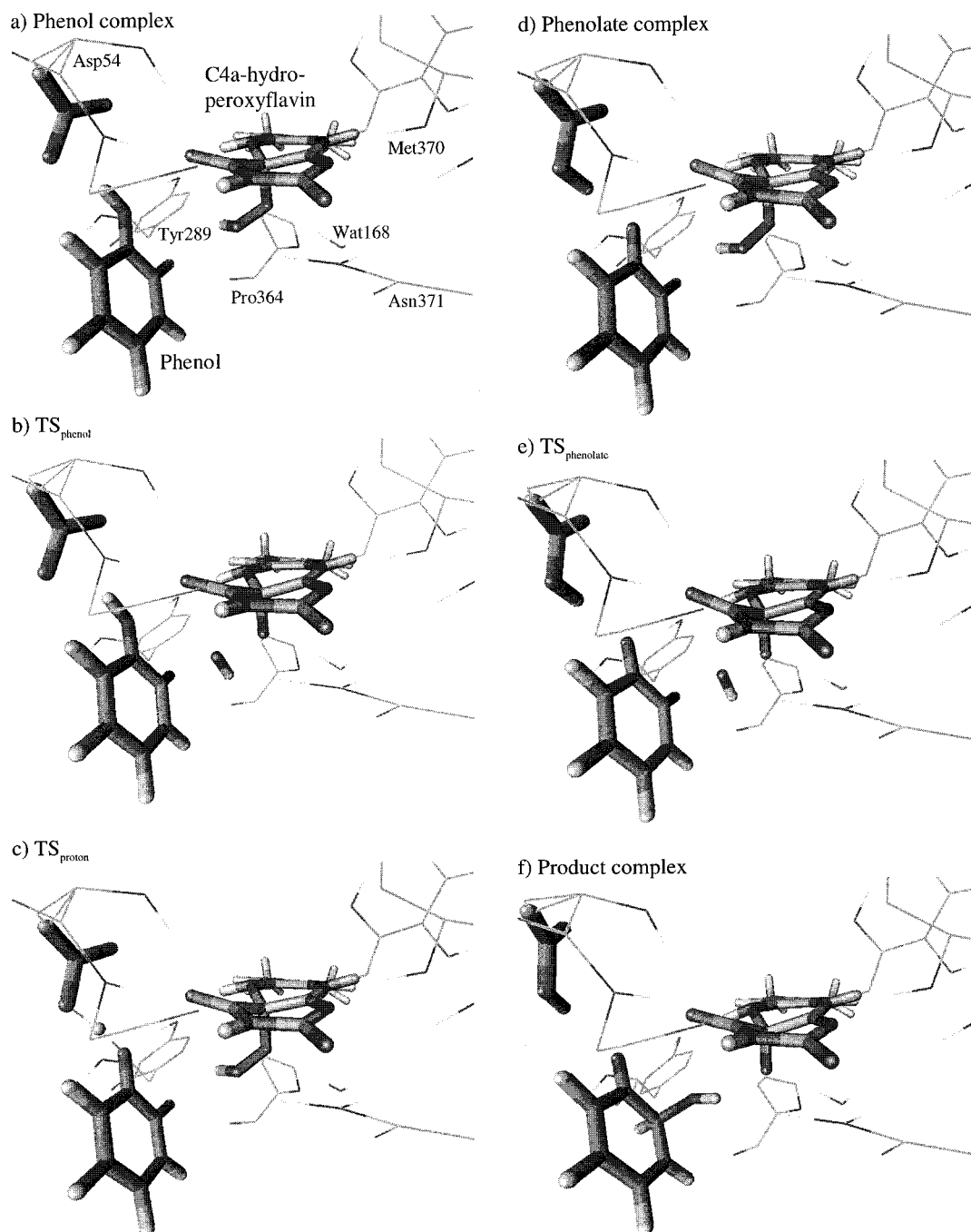
labeled "unstable" in Figure 3). Rather, the positively charged cyclohexadienol is very unstable, and the H1′ proton would spontaneously shift to Asp54, without crossing an energy barrier. The alternative reaction pathway first encounters an energy barrier for proton transfer of only 6 kcal/mol after which the barrier for hydroxylation is 24 kcal/mol. Thus, the potential energy surface suggests the latter reaction pathway to be most favorable. The hydroxylation of phenolate (after the H1′ proton has been transferred to Asp54) does result in a stable product. Analysis of the bond lengths (Table 1) and the Mulliken charge distribution (Supporting Information) in the QM system for the various intermediate structures indicates that this product of the hydroxylation of phenolate is a cyclohexadienone. This follows, first of all, from a decrease in the C2′−C3′, C4′−C5′, and C1′−O1′ bond distances and a lengthening of the other substrate C−C bonds (Table 1, columns 5−7). Second, a significant decrease in the negative charge on O1′ (from −0.64*e* to −0.35*e*) indicates its transition from a deprotonated hydroxyl oxygen in the phenolate complex to a carbonyl oxygen in the product complex. In total, −1*e* charge is transferred from the substrate to the flavin cofactor. The resulting formal charge on the proximal oxygen is delocalized over the flavin ring. Altogether, the results for the hydroxylation of phenolate are in agreement with an electrophilic aromatic substitution type of mechanism.

Active-Site Interactions. Various results obtained from the present QM/MM model provide information about the interactions between the QM and MM regions, and how these interactions change during reaction processes. Table 1 (lower section) lists some important interatomic distances between QM and MM atoms, which represent hydrogen bonds in the various intermediates. Changes in the hydrogen bond distances indicate changes in the strength of these interactions, which are often caused by the changes in the electronic structure (e.g., charge distribution; details available in the Supporting Information) of the QM system. More quantitative information about the interactions between MM residues and the QM system was obtained from the results of the energy decomposition analyses, presented in Figures 5 and 6. These analyses provide approximate values for the effects of individual amino acids and water molecules on the change in energy upon transfer of the H1′ proton to Asp54 (Figure 5) and on the energy barrier (Figure 6a) and the overall energy change (Figure 6b) for hydroxylation

of phenolate. The QM/MM energy differences between the phenol and phenolate complex (Figure 5), between the phenolate complex and the TS$_{phenolate}$ (Figure 6a) and between the phenolate and product complex (Figure 6b), are plotted as a function of the amino acids included (in order of the distance of their center of mass (COM) to the center of the simulation system). Combining the data from Table 1 and Figures 5 and 6, a number of catalytic features of PH with respect to hydroxylation and proton transfer to Asp54 are identified.

First, a hydrogen bond interaction appears to exist between the hydroxyl hydrogen of Tyr289 and O1′ of phenol in the initial phenol complex (Table 1). This hydrogen bond is expected to be important for binding the substrate. Upon proton transfer to Asp54 leading to the formation of the phenolate complex, the hydrogen bond distance between Tyr289 and the O1′ of the substrate decreases from 1.88 to 1.80 Å, indicating a stabilization of the negative charge on O1′ (which increases from −0.35*e* to −0.64*e* according to Mulliken analysis). This interpretation is in line with the effect of Tyr289 on the energy change upon proton transfer as observed in the energy decomposition analysis for this step presented in Figure 5. The analysis indicates a stabilization of the phenolate complex by Tyr289 by about 3 kcal/mol, relative to that of the phenol complex. During subsequent hydroxylation of the phenolate, the hydrogen bond distance between Tyr289 and O1′ of the substrate increases, which can be explained by the fact that the negatively charged hydroxyl oxygen (−0.64*e* by Mulliken analysis) formally becomes a neutral carbonyl oxygen (−0.35*e* by Mulliken analysis) which forms a weaker hydrogen bond with Tyr289. This is in accordance with Figure 6, which indicates that Tyr289 increases the energy barrier for hydroxylation by about 3 kcal/mol (Figure 6a) and makes the overall energy change of the reaction approximately 7 kcal/mol less negative (Figure 6b).

A second remarkable interaction can be identified between the backbone carbonyl oxygen of Pro364 and the Od-Hd moiety. This interaction appears to exist specifically in the transition state for hydroxylation. Table 1 indicates that the interatomic distance between Hd and the carbonyl oxygen of Pro364 is much smaller in both transition states for hydroxylation compared to those in the reactant and product complexes. By comparing Figure 4d, e, and f it is apparent that the Od−Hd moiety rotates almost 180° during its transfer from cofactor to phenolate. In

Hydroxylation of Phenol and Halogenated Derivatives

J. Am. Chem. Soc., Vol. 122, No. 36, 2000 8733

a) Phenol complex

Asp54

C4a-hydro-
peroxyflavin

Met370

Tyr289

Wat168

Pro364

Asn371

Phenol

b) TS$_{\text{phenol}}$

c) TS$_{\text{proton}}$

d) Phenolate complex

e) TS$_{\text{phenolate}}$

f) Product complex

Figure 4. Optimized active-site structures (showing QM atoms with thick bonds, MM atoms in thin lines using VMD[44]) of (a) the phenol C4a-hydroperoxyflavin complex, (b) the transition state for direct hydroxylation of phenol (TS$_{\text{phenol}}$), (c) the transition state for proton transfer to Asp54 (TS$_{\text{proton}}$), (d) the phenolate C4a-hydroperoxyflavin complex, (e) the transition state for hydroxylation of the phenolate (TS$_{\text{phenolate}}$), and (f) the product of hydroxylation.

the transition state the OH moiety points toward the backbone oxygen of Pro364. Through this interaction, which is observed only in the transition state, the (partially) negatively charged carbonyl oxygen of Pro364 may stabilize the partial positive charge on Hd in the transition state ($0.23e$ by Mulliken analysis). The energy decomposition analysis for the hydroxylation step indeed indicates that Pro364 lowers the energy barrier for the hydroxylation step by about 3 kcal/mol.

A third important QM−MM interaction involves a crystal water molecule, Wat168. This water molecule remains in the position it occupies in the crystal structure during the initial equilibration of the solvent. This solvent molecule donates a hydrogen bond to the proximal oxygen of the peroxide moiety (Op) of the flavin cofactor. The Wat168−Op hydrogen bond

becomes shorter upon hydroxylation of the phenolate, indicating that it increases in strength. (Table 1, columns 5 to 7). This suggests that Wat168 plays a role in stabilizing the negative charge on the proximal oxygen Op of the cofactor (the Mulliken charge on Op increases from $-0.19e$ in the phenolate complex to $-0.33e$ in the C4a-hydroxyflavin product). The stabilizing effect of Wat168 on the C4a-hydroxyflavin anion is also apparent from the decomposition analysis which indicates that Wat168 makes the hydroxylation reaction 6 kcal/mol more favorable (Figure 6a and b).

Five other hydrogen bond interactions, between N1, O2, and O4 of the flavin ring and polar hydrogen atoms of residues Asp54, Gly55, Met370, and Asn371, appear to increase in strength (i.e., the distances become shorter, Table 1) upon

Table 1. Relative Energy (kcal/mol) of the Various Intermediates and Approximate Transition States on the Calculated Potential Energy Surface for the QM/MM Model, and a Selection of Interatomic Distances (Å) between QM Atoms and between QM and MM Atoms[a]

	phenol complex	TS$_{phenol}$	TS$_{proton}$	phenolate complex	TS$_{phenolate}$	product complex
energy	0	36.17	6.0	−0.48	23.22	−59.40
C4a−Op	1.48	1.38	1.48	1.48	1.40	1.31
Op−Od	**1.28**	**1.76**	**1.28**	**1.28**	**1.63**	**2.94**
Od−C6′	**3.11**	**1.99**	**3.08**	**3.10**	**2.13**	**1.41**
C6′−C1′	1.41	1.42	1.42	1.43	1.44	1.53
C1′−C2′	1.41	1.42	1.42	1.43	1.45	1.47
C2′−C3′	1.39	1.38	1.38	1.38	1.37	1.35
C3′−C4′	1.40	1.41	1.40	1.40	1.42	1.45
C4′−C5′	1.40	1.38	1.40	1.40	1.38	1.34
C5′−C6′	1.39	1.42	1.39	1.38	1.41	1.49
C1′−O1′	1.36	1.34	1.32	1.29	1.27	1.24
O1′−H1′	**0.99**	**1.00**	**1.22**	**1.92**	**1.98**	**2.14**
H1′−OD1	**1.87**	**1.83**	**1.19**	**0.99**	**0.99**	**0.98**
CG−OD1	1.27	1.27	1.30	1.34	1.34	1.35
CG−OD2	1.27	1.27	1.25	1.24	1.24	1.23
Tyr289-H−O1′	1.88	1.85	1.87	1.80	1.82	2.06
Pro364-O−Hd	2.60	1.99	2.79	3.07	2.14	2.89
Wat168-H−Op	2.10	2.09	2.11	2.12	2.09	2.01
Asp54-H−O4	2.23	2.17	2.10	2.04	1.99	1.99
Gly55-H−O4	2.44	2.19	2.32	2.31	2.16	2.13
Met370-H−N1	2.16	2.16	2.15	2.17	2.18	2.12
Asn371-H−O2	2.77	2.71	2.75	2.82	2.80	2.65
Asn371-HD−O2	2.25	2.11	2.22	2.25	2.13	2.08

[a] Energies are given relative to the energy of the phenol complex. The distances subject to reaction coordinate restraints are shown in bold face. Atom labeling as in Figure 1.
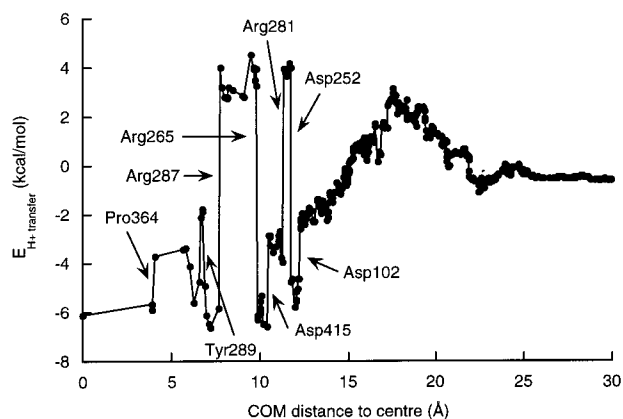
Figure 5. Decomposition analysis illustrating the contribution of individual MM residues to the QM/MM energy difference between the phenol C4a-hydroperoxyflavin complex and the phenolate C4a-hydroperoxyflavin complex, E(phenolate complex) − E(phenol complex).

hydroxylation. Thus, these interactions may stabilize, to some extent, the increasing negative charge on the flavin ring, especially on the N1, O2, and O4 atoms (details in the Supporting Information), upon formation of the deprotonated C4a-hydroxyflavin product of the hydroxylation step. Accordingly, small favorable effects (i.e., making the reaction energy more negative) of the residues Asp54, Met370, and Asn371 on the hydroxylation step are observed in the energy decomposition analysis (Figure 6b).

The strongest effects on the energy changes upon proton transfer and hydroxylation are observed from charged residues (Figures 5 and 6). Considerable redistributions of charge accompany the proton transfer and the hydroxylation reactions. Therefore, the effects (mainly electrostatic) of charged residues depend on the formal charge and the position of the residue with regard to the QM system in which charge redistributions occur. These strong effects, at relatively long distances (e.g., Asp102, Asp252, and Asp415), indicate that the nonbonded
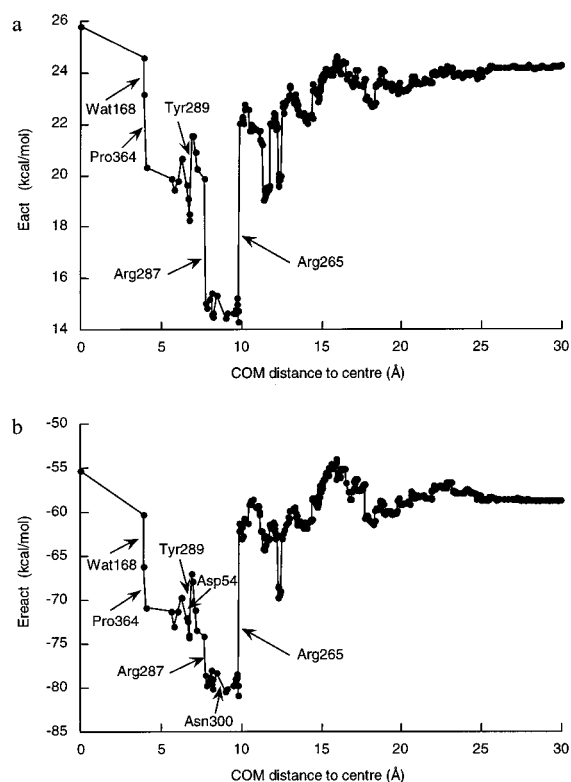
Figure 6. Decomposition analysis illustrating the contribution of individual MM residues to the QM/MM energy difference (a) between the phenolate C4a-hydroperoxyflavin complex and the transition state for hydroxylation, E(TS$_{phenolate}$) − E(phenolate complex), and (b) between the phenolate C4a-hydroperoxyflavin complex and the product of hydroxylation, E(product complex) − E(phenolate complex).

cutoff distance must be chosen with care. The nonbonded cutoff function applied in the present model scales the interactions down to zero over a relatively broad range (between 11 and 16 Å). This seems, in retrospect, to be a reasonable treatment of the nonbonded interactions in this system.

Table 2. Results of Transition State Optimizations in Vacuum for the Model System for Hydroxylation Presented in Figure 2A[a]

transition states:	d(Op−Od) (Å)	d(Od−C6′) (Å)	ΔH_{TS} (kcal/mol)	imaginary frequency
AM1	1.68	1.98	25.12	725i
HF/6-31+G(d)	1.87	1.92	49.28	983i
B3LYP/6-31+G(d)	1.93	1.97	9.84	391i
B3LYP/6-311+G(2d,p)// B3LYP/6-31+G(d)	id.	id.	10.02	
MP2/6-31+G(d)	1.86	1.99	5.06	
MP4/6-31+G(d)// MP2/6-31+G(d)	id.	id.	11.92	

[a] ΔH_{TS} is the enthalpy of the transition state relative to the total enthalpy of the separate (optimized) reactants. Note: The HF, MP2, and MP4 enthalpies were calculated from the corresponding energies by applying an unscaled thermal correction based on HF/6-31+G(d) frequency calculations. Likewise, the B3LYP enthalpies are based on B3LYP/6-31+G(d) frequency calculations.

Overall, the energy change upon proton transfer is almost zero within the complete protein model, whereas it is −6 kcal/mol for the QM atoms only (Figure 5). This indicates that the electrostatic environment of the enzyme favors the phenol complex with Asp54 deprotonated, relative to the phenolate complex. The energetics of the hydroxylation are relatively little affected by the protein (Figure 6a and b).

Gas-Phase Calculations on Small Model Systems for the Hydroxylation Reaction and for the Proton Transfer from Phenol to Asp54. A possible source of inaccuracy in the calculated potential energy surface (Figure 3) is the fact that it is based on the semiempirical AM1 method. To validate the use of AM1 for the QM system, and to obtain insight into how the energy surface may change on going to a higher level of theoretical treatment, gas-phase calculations were performed on small model systems for the two reaction coordinates. The performance of AM1 for these models was tested by comparison to results at higher levels of quantum chemical theory. First, transition-state optimizations were performed on the model system for hydroxylation as shown in Figure 2a. Some quantitative differences between the results at the various levels of theory are observed. Table 2 presents the interatomic distances for the bonds which are broken (Op−Od) and formed (Od−C6′) in the calculated transition states at different levels of theory. Comparison of the geometries optimized at the AM1, HF/6-31+G-(d), MP2/6-31+G(d), and B3LYP/6-31+G(d) levels indicates that AM1 underestimates the Op−Od bond distance in the TS by about 0.2 Å, whereas it performs well for the Od−C6′ distance. The AM1 results for the Op−Od and Od−C6′ distances (1.68 and 1.98 Å, Table 2) in the small TS model in gas phase differ slightly from the corresponding values in the approximate QM/MM transition state for hydroxylation of phenolate (1.63 and 2.13 Å, Table 1, column 6), possibly indicating that the flavin ring does affect the reactive properties of the peroxide moiety (as would be expected).

Table 2 also presents the TS energies relative to the separate reactants, calculated at different levels of theory. The MP4 or B3LYP methods are the highest levels of theory used, and the results obtained at these levels serve as the reference values. Although the AM1 result appears better than the HF/6-31+G-(d) outcome, AM1 overestimates the activation energy for hydroxylation, by possibly more than 10 kcal/mol. This may explain the apparent discrepancy between the absolute value of the QM/MM energy barrier and the experimental rate constant. Neglecting entropic contributions, the experimental rate constant of 470 min^{-1} would correspond to a barrier of about 16 kcal/mol. The difference between this expected barrier and the calculated QM/MM barrier of 23.7 kcal/mol is

Table 3. Relative Energies in kcal/mol of the Phenol Acetate Complex, the Transition State for Proton Transfer (Figure 2b) and the Phenolate Acetic Acid Complex in the Gas Phase at the AM1, HF/6-31+G(d), MP2/6-31+G(d)//HF/6-31+G(d), and the B3LYP/6-31+G(d)//HF/6-31+G(d) Levels

	phenol complex	TS	phenolate complex
AM1	0	4.56	−0.73
HF/6-31+G(d)	0	7.66	6.96
MP2/6-31+G(d)//HF/6-31+G(d)	0	4.29	6.21
B3LYP/6-31+G(d)//HF/6-31+G(d)	0	2.18	4.67

within the error of AM1 indicated above on the basis of the test calculations.

The AM1 method was also tested for the proton transfer from phenol to acetate (as a model for Asp54) in the gas phase. Geometry optimizations were performed at the AM1 and HF/6-31+G(d) levels for the phenol acetate complex, the transition state (represented in Figure 2b) and the phenolate acetic acid complex. The energies of the various species at the AM1, HF/6-31+G(d), MP2/6-31+G(d)//HF/6-31+G(d), and B3LYP/6-31+G(d)//HF/6-31+G(d) levels are presented in Table 3, relative to the energy of the phenol acetate complex. AM1 predicts the phenol−acetate complex to be less stable than the phenolate−acetic acid complex. In contrast, the ab initio and B3LYP methods predict the phenol−acetate complex to be more stable than the phenolate−acetic acid complex, as would be expected on the basis of the fact that acetic acid is a stronger acid than phenol. The error of about 6 kcal/mol in AM1 seems to be due to a known overestimation of the proton affinity of carboxylate by AM1.[34]

It should be noted that in the QM/MM model Asp54 is represented by formate in the QM system rather than by acetate. At the AM1 level the proton affinity of acetate (354.8 kcal/mol) and formate (355.1 kcal/mol) are very similar, and thus, for reasons of efficiency, formate was chosen to represent Asp54 in the QM/MM model. At the MP2/6-31+G(d) and B3LYP/6-31+G(d) levels the proton affinity of acetate (346.57 and 349.42 kcal/mol, respectively) differs by about 5 kcal/mol from the proton affinity of formate (341.87 and 344.55 kcal/mol, respectively) and was chosen to be a more realistic representation of Asp54 in the gas-phase model. However, because of the similar proton affinities of formate and acetate at the AM1 level, the comparison of the results for the acetate complex at various levels can be extrapolated to the QM/MM model. Thus, the comparison of AM1 with the higher levels of theory in Table 3 suggests that the proton transfer from phenol to Asp54 in the active site of PH may be somewhat more unfavorable than it appears from the calculated potential energy surface, due to an overestimation of the proton affinity of Asp54 in the QM/MM model.

In summary, the results of the test calculations in gas phase suggest some corrections to the potential energy surface presented in Figure 3 and the energies given in Table 1. The phenolate complex may be about 6 kcal/mol more unfavorable relative to the phenol complex. Furthermore, the energy barrier for the subsequent hydroxylation may be lower. From a qualitative point of view, however, the conclusions drawn from the potential energy surface remain unchanged. The approximate transition state for hydroxylation of the phenolate in the QM/MM model (formed upon proton transfer) is 13 kcal/mol lower than the transition state for direct hydroxylation of the phenol. Even if a correction of 6 kcal/mol on the energy change upon

(34) Mulholland, A. J.; Richards, W. G. *J. Phys. Chem. B* **1998**, *102*, 6635−6646.

Table 4. Experimental Rate Constants for Overall Conversion of a Series of Halogenated Phenols by Phenol Hydroxylase,[1] and Calculated Energy Barriers $E_{act(1)}$ for the Electrophilic Attack of the C4a-hydroperoxyflavin on the C6′ of the Phenolate Substrates[a]

substrate	k_{cat} (min^{-1})	$E_{act(1)}$ (kcal/mol)	r_{OH}(TS) (Å)	E_{act2} (kcal/mol)	r_{OH}(TS) (Å)
phenol	470	23.70	(−0.50)		
2-F-phenol (6-F)	150	25.68	(−0.49)	26.32	(−0.50)
3-F-phenol (5-F)	280	24.69	(−0.49)	25.35	(−0.49)
4-F-phenol	470	24.58	(−0.49)		
2,3-F$_2$-phenol (5,6-F$_2$)	90	26.35	(−0.47)	27.23	(−0.49)
2,4-F$_2$-phenol (4,6-F$_2$)	190	25.98	(−0.47)	27.52	(−0.47)
2,5-F$_2$-phenol (3,6-F$_2$)	150	27.25	(−0.47)	27.29	(−0.48)
3,4-F$_2$-phenol (4,5-F$_2$)	390	25.56	(−0.47)	26.09	(−0.47)
3,5-F$_2$-phenol	280	26.37	(−0.47)		
2,3,4-F$_3$-phenol (4,5,6-F$_3$)	150	26.91	(−0.44)	28.56	(−0.46)
2,3,5-F$_3$-phenol (3,5,6-F$_3$)	70	28.09	(−0.45)	28.42	(−0.47)
3,4,5-F$_3$-phenol	210	27.26	(−0.45)		
2,3,5,6-F$_4$-phenol	50	30.04	(−0.44)		
2,3,4,5,6-F$_5$-phenol	40	30.88	(−0.41)		
3-Cl,4-F-phenol (5-Cl,4-F)	190	24.89	(−0.45)	26.52	(−0.47)
4-Cl,3-F-phenol (4-Cl,5-F)	270	24.44	(−0.45)	24.85	(−0.47)

[a] In case of asymmetric substrates a second energy barrier E_{act2} is calculated for the attack of the C4a-hydroperoxyflavin on the C6′ of the substrates with the alternative substituent positions (in brackets, column 1), representing the reaction with the substrates in the alternative binding orientation. Columns 4 and 6 present the reaction coordinate value at the transition state, r_{OH}(TS), with $r_{OH} = d(Op-Od) - d(Od-C6')$.

proton transfer from phenol to Asp54 were to be extrapolated to both transition states for hydroxylation (which might be an overcorrection), the potential energy surface would still favor a reaction mechanism involving initial proton transfer based on a residual difference of about 7 kcal/mol between the transition states of hydroxylation of the phenol and phenolate complexes.

Computation of Energy Barriers with Halogenated Substrates. In subsequent calculations, the energy barrier for hydroxylation of the phenolate complex, after initial proton transfer, was also determined for a number of substituted substrates. The structures of the phenolate and transition state complexes calculated for the substrate analogues were in all cases comparable to those found for the native phenolate. The energy barriers and reaction coordinate values of the approximate transition states for the various substrates are listed in Table 4. For asymmetric substrates the calculations were performed for the two possible binding orientations in the active site. Overall, the substituents increase the energy barrier. This is likely to be due to the electronegative character of the substituents, which withdraw electron density from the aromatic ring, lowering the reactivity of the substrate for electrophilic attack by C4a-hydroperoxyflavin.[1] Fluorine substituents on the reacting C6′ center seem to have a stronger effect on the barrier than fluorine substituents on other positions. The fluorine substituents on this position may affect the energy involved in changing the hybridization of C6′ from sp^2 to sp^3 and in loss of aromaticity upon hydroxylation; another possibility is that a fluorine substituent at this position sterically hinders the reaction. The substitutions (except for those on C6′) cause a shift of the TS geometry toward the product geometry, that is, r_{OH}(TS) becomes less negative, which corresponds to a decrease in Od−C6′ (varying between 2.09 and 2.14 Å) distance and an increase in Op−Od distance (varying between 1.62 and 1.70 Å).

Correlation of Calculated Barriers with Experimental Rate Constants. On the basis of the hypothesis that the electrophilic attack of the C4a-hydroperoxyflavin on the substrate is rate-limiting in the overall reaction cycle of PH, the calculated energy barriers for the different substrates were compared to the experimental rate constants for their overall conversion by PH.[1] For the symmetric substrates, indeed an excellent linear correlation ($R = 0.98$) was found between the logarithm of the experimental rate constants and the calculated energy barriers for the reaction of the C4a-hydroperoxyflavin with the substrate. For the asymmetric substrates slightly
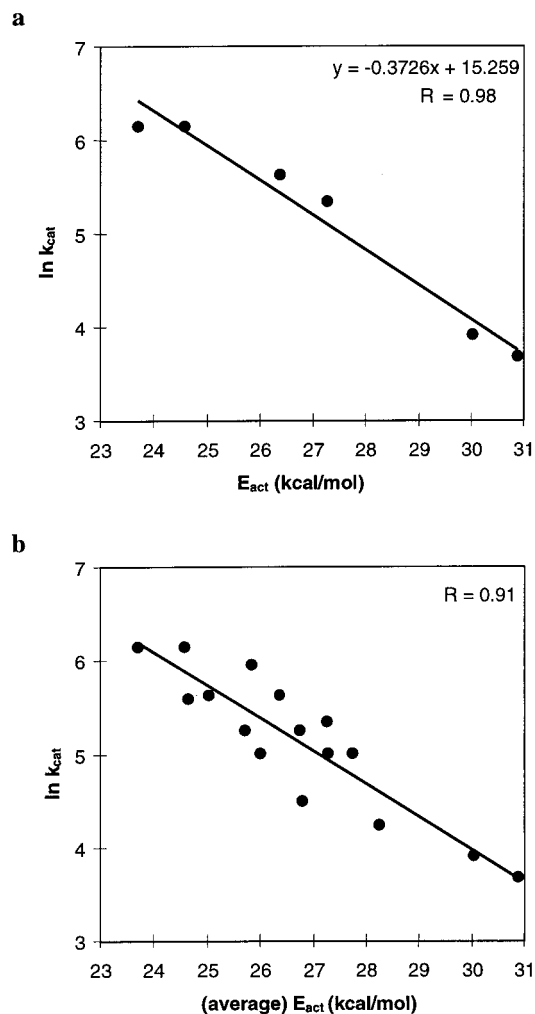
Figure 7. Linear correlations between the natural logarithm of the experimental rate constants (min^{-1}) for overall conversion of symmetric phenol derivatives[1] and the (average) calculated energy barriers (E_{act}) obtained for (a) the symmetric substrates only and (b) all substrates.

different energy barriers are obtained for the two possible orientations in the active site (Table 4). Figure 7b shows that the average energy barriers for the asymmetric substrates, together with the energy barriers for the symmetric substrates,

also correlate well ($R = 0.91$) with the natural logarithm of the experimental rate constants for overall hydroxylation.

An attempt to derive apparent energy barriers, taking into account experimental product ratios[1] for the various asymmetric substrates, did not improve the correlation (details are available in the Supporting Information). This may suggest that the differences in energy barriers for two different substrate orientations do not provide significant information on the regioselectivity of the reaction.

Discussion

The potential energy surface obtained in the present study is based on an energy minimization approach, which is also referred to as adiabatic mapping.[35] This approach does not include contributions of the protein dynamics, which may involve multiple conformational substates.[36,37] Instead, it is based on a single conformation, which is expected to be representative for the reacting enzyme The conformation used is derived from the crystal structure of the oxidized enzyme−substrate complex, with the flavin in the "in" position.[11] Analogous to the case of PHBH, the reactive C4a-hydroperoxyflavin is in a similar position[19] and the protein structure is not expected to change significantly upon hydroxylation.[10,38,39]

The observed correlation, between the calculated QM/MM energy barriers and the logarithm of the experimental rate constants of overall conversion by PH, indicates that the QM/MM model indeed provides an appropriate description of the rate-limiting step (at 25 °C and pH 7.6) in the reaction cycle of PH. The analysis of the changes in geometry and charge, along the reaction coordinate for hydroxylation of the phenolate, indicates that the (validated) QM/MM model is in line with an electrophilic aromatic substitution which results in the formation of a hydroxycyclohexadienone as the initial product. Although the calculated energy barriers for hydroxylation are somewhat too high, as suggested by the gas-phase results on the small model system (Table 2), the results show that the barriers are useful in a relative way. The correlation for a broad range of substrates, including not only fluorinated phenols, but also chlorinated phenols, holds out the possibility of predicting conversion rates of other substrates by phenol hydroxylase. It shows the potential utility of the QM/MM method for quantitative structure activity relationship (QSAR) studies.

The present simulation provides new insight into the activation of the phenolic substrate by proton transfer from the hydroxyl moiety of the substrate to a potential active site base, Asp54. NMR experiments indicate that the substrate binds to the oxidized PH enzyme in its neutral protonated state.[16] Apparently, the active-site base Asp54, which appears to form a hydrogen bond with the hydroxyl moiety of the substrate on the basis of the crystal structure, does not deprotonate the substrate at that stage in the reaction cycle. The QM/MM model suggests that, further on in the reaction cycle, the electrophilic attack of the C4a-hydroperoxyflavin on the substrate occurs after a proton has been transferred from phenol to Asp54.

The first question that one may address is at what point in the reaction cycle the proton is transferred from phenol to Asp54.

If the QM/MM potential energy surface obtained in the present simulation study (Figure 3) is corrected for an overestimation (by up to approximately 6 kcal/mol) of the Asp54 proton affinity by AM1, which appears from the comparison to higher level calculations (Table 3), the phenolate complex would be almost 6 kcal/mol higher in energy than the phenol complex. This suggests that, in the C4a-hydroperoxyflavin intermediate of the PH reaction cycle, the proton may still be preferentially present on the phenolic substrate. However, although the initial proton-transfer step might be energetically unfavorable, the lower energy barrier of the subsequent electrophilic attack seems to more than compensate for this. In kinetic terms this means that, although only a small fraction of the substrate is in a deprotonated state, the subsequent hydroxylation reaction proceeds so much faster in this deprotonated state that this pathway prevails over the hydroxylation of the substrate in its protonated state.

This idea about substrate activation in PH, that is, that it occurs just before the hydroxylation takes place, is different from the mechanism of PHBH, in which substrate is deprotonated directly upon binding in the active site (before the flavin cofactor is reduced).[13,14,18] Thus, the second question that comes up is what would be the advantage of keeping phenol neutral during the first steps in the reaction cycle of PH (whereas in PHBH substrate is deprotonated directly after binding)? Related to the fact that the hydroxyl moiety of phenol is the only polar group of the molecule to be involved in orientating the substrate in the active site, one could speculate that the substrate might be more specifically or efficiently bound (and orientated) by the two hydrogen bonds with Asp54 and Tyr289 when phenol is present in its neutral state. In PHBH, the *p*-hydroxybenzoate substrate is orientated by hydrogen bonding of the carboxyl moiety as well, which makes the role of the hydroxyl moiety in substrate binding/orientation less important. In this context, it is interesting to note that, by structural alignment of the phenol hydroxylase and *p*-hydroxybenzoate hydroxylase crystal structures, the hydroxyl moiety of phenol in phenol hydroxylase binds at the site where the carboxyl moiety (instead of the hydroxyl moiety) of *p*-hydroxybenzoate binds in *p*-hydroxybenzoate hydroxylase.

In combination with previous work,[10] the results of the present study allow a detailed comparison of the catalytic features of the active sites of the two related enzymes, PH and PHBH, with respect to the hydroxylation step. The observed changes in charge distribution and bond distances upon hydroxylation are very similar in the present simulation of PH and the previous simulation of PHBH, which supports the proposal that the mechanism of hydroxylation is similar in both enzymes. In addition, some common active-site interactions appear to play a role in both hydroxylation reactions. A crystal water molecule is present at a similar position in the active sites of both enzymes structures. In the simulations of both enzymes, this water molecule donates a hydrogen bond to the proximal oxygen (Op) of the C4a-hydroperoxyflavin cofactor, which results in a stabilization of the increasing negative charge on Op. Catalytic effects of bound water molecules, by stabilizing transient negative charges, have been recently reported for other enzymes too,[7,40] which may indicate their general importance. A second comparison can be made for the role of a tyrosine (Tyr289 in PH and Tyr201 in PHBH) which forms a hydrogen bond with the hydroxyl moiety of the substrate. In PHBH, Tyr201 is known to be directly involved in deprotonating the substrate,[13,14] as the first step in a proton channel to transport the proton out of

(35) McCammon, J. A.; Harvey, S. C. *Dynamics of Proteins and Nucleic Acids*; University Press: Cambridge, 1987.

(36) Frauenfelder, H.; Sligar, S. G.; Wolynes, P. G. *Science* **1991**, *254*, 1598−1603.

(37) Kurzynski, M. *Prog. Biophys. Mol. Biol.* **1998**, *69*, 23−82.

(38) Schreuder, H. A.; Van der Laan, J. M.; Hol, W. G.; Drenth, J. *J. Mol. Biol.* **1988**, *199*, 637−648.

(39) Schreuder, H. A.; Prick, P. A. J.; Wierenga, R. K.; Vriend, G.; Wilson, K. S.; Hol, W. G. J.; Drenth, J. *J. Mol. Biol.* **1989**, *208*, 679−696.

(40) Zheng, Y. J.; Ornstein, R. L. *J. Am. Chem. Soc.* **1997**, *119*, 648−655.

the active site.[18,41] The present study indicates that in PH substrate may be deprotonated by Asp54 rather than Tyr289. Furthermore, the position of Tyr289 in the active site of PH is completely different from the position of Tyr201 in PHBH. (It is, however, comparable in position to Tyr222 in PHBH, which binds the substrate carboxylate.) Despite these important differences, one effect of Tyr289 in PH and Tyr201 in PHBH seems to be similar, on the basis of the comparison of the present and previous QM/MM simulations, respectively: it appears to stabilize the activated substrate by forming a hydrogen bond with the deprotonated hydroxyl moiety. In both simulations, this hydrogen bond becomes weaker along the reaction coordinate of the hydroxylation step, which results in a slight unfavorable effect on this reaction step.

A third common feature is the catalytic function of the backbone carbonyl moiety of a conserved proline residue, that is, Pro293 in PHBH and Pro364 in PH, which is similarly oriented toward the FAD cofactor in both structures. The positions of these proline residues are also identical in the (structural) alignment of both proteins.[11] The (partially) negatively charged carbonyl oxygen specifically stabilizes the transition state by a hydrogen bond interaction with the somewhat positively charged Od−Hd moiety in the process of being transferred from the cofactor to the substrate. It is an interesting question whether the catalytic feature of the backbone carbonyl observed in the simulation studies on PHBH and PH could be of a more general significance. A backbone carbonyl oxygen has a relatively large (partial) negative charge due to π-interaction with the free electron pair on the nitrogen through the peptide bond. The backbone carbonyl moiety is therefore a suitable candidate for stabilizing positively charged groups.

Furthermore, the advantage of a (carbonyl) backbone group is that its position and orientation is relatively well defined (i.e., restricted). This allows the carbonyl moiety to be tightly oriented, such that it can specifically stabilize a transition state, as appears to be the case in the present simulation study. One could argue about the significance of a proline residue being present at this specific position in an active site loop, in both PH and PHBH. It is interesting to note that this proline residue is part of the FAD fingerprint motif in the flavoprotein monooxygenases.[42,43] It is tempting to speculate that the suggested catalytic role of the backbone carbonyl could be one of the reasons for the conservation of a proline residue at this position. The proline residue, due to its cyclic structure, might induce and restrain a specific conformation of the backbone at this position and thus keep the backbone carbonyl moiety in the right orientation for its stabilizing interaction in the transition state.

Supporting Information Available: Table of atomic Mulliken charges; derivation of apparent energy barriers for the asymmetric substrates taking into account experimental product ratios[1](PDF). This material is available free of charge via the Internet at http://pubs.acs.org.

(41) Gatti, D. L.; Entsch, B.; Ballou, D. P.; Ludwig, M. L. *Biochemistry* **1996**, *35*, 567−578.

(42) Eppink, M. H.; Schreuder, H. A.; Van Berkel, W. J. H. *Protein Sci.* **1997**, *6*, 2454−2458.

(43) Dimarco, A. A.; Averhoff, B. A.; Kim, E. E.; Ornston, L. N. *Gene* **1993**, *125*, 25−33.

(44) *VMD*, v1.2b; Theoretical Biophysics Group, University of Illinois and Beckman Institute: Chicago, IL, 1996.